PHILOSOPHICAL TRANSACTIONS OF THE ROYAL SOCIETY A MATHEMATICAL, PHYSICAL & ENGINEERING SCIENCES

An astronomical tuning strategy for Pliocene sections: implications for global-scale correlation and phase relationships

Steven C. Clemens

Phil. Trans. R. Soc. Lond. A 1999 **357**, 1949-1973
doi: 10.1098/rsta.1999.0409

THE ROYAL SOCIETY

An astronomical tuning strategy for Pliocene sections: implications for global-scale correlation and phase relationships

By Steven C. Clemens

Box 1846, Department of Geological Sciences, Brown University, Providence, RI 02912-1846, USA

Astronomical tuning plays a central role in developing the chronostratigraphy of marine sediment sections. For Pleistocene sections, tuning is typically accomplished by matching the 41 and 23 ka components of oxygen isotopes (δ^{18}O-41, δ^{18}O-23) to orbital obliquity and precession with constant phase lags of 69° and 78°, respectively (depleted δ^{18}O-41 lags maximum obliquity by 7.8 ka, while depleted δ^{18}O-23 lags minimum precession by 5 ka). This approach places all records on the same time-scale relative to one another and relative to insolation forcing because Pleistocene δ^{18}O is globally correlative. Thus, lead and lag relationships among climate variables measured at globally distributed sites can be assessed in an effort to understand the underlying physics of climate change. For Pleistocene sections, variables such as dust content, magnetic susceptibility, colour reflectance, and gamma-ray attenuation porosity evaluator (GRAPE) are typically tuned directly to precession or to a precession-dominated insolation target. Unlike Pleistocene δ^{18}O, these variables are not globally correlative and few have unambiguous models linking them to insolation forcing. Consequently, the capacity to compare Pliocene lead and lag relationships among climate variables from different sites is considerably diminished, as is the capacity to evaluate the climate response to orbital forcing. Here a Pliocene tuning strategy is presented which builds on the precession-based approach by incorporating a final tuning step involving δ^{18}O-41. Results from application to Site 659 and the Mediterranean *Rossello* Composite Section suggest qualified success. Application to other Pliocene sections is required to verify the utility of this astronomical tuning approach.

Keywords: astronomical tuning; Pliocene time-scale; Milankovitch cyclicity; insolation forcing; non-stationary phase response

1. Introduction

Research over the past 15 years has produced significant advances in the development of the Plio-Pleistocene astronomical time-scale (Hilgen 1991*a*, *b*; Hilgen *et al*. 1993; Lourens *et al*. 1996; Raymo *et al*. 1989; Ruddiman *et al*. 1986; Shackleton *et al*. 1990, 1995*a*; Tiedemann & Franz 1998; Tiedemann *et al*. 1994). Much of this work has focused on improving the accuracy of the geomagnetic polarity time-scale (GPTS) and the associated biostratigraphic datums; two primary means of establishing marine and terrestrial chronostratigraphy. Successful application in this respect requires only that tuned sediment sections be stratigraphically complete and that orbital-scale (41 and 23 ka) cycles be identified and counted correctly. For example,

the onset of the Sidufjall {C3n.3n (o)} is dated at 4.47 Ma using the Berggren *et al*. (1985) time-scale. Astronomical tuning efforts place this event at 4.878 Ma on the Shackleton *et al*. (1995*a*) time-scale, 4.890 Ma on the Hilgen (1991*b*) time-scale, and 4.896 Ma on the Lourens *et al*. (1996) time-scale. Thus, astronomical tuning has revised the age of this event of the order of 400 000 years older. If one were to average the three astronomical estimates, then the resulting age would be 4.888 ± 0.018 Ma ($n = 3, 2\sigma$). Based on these three time-scales, the average 2σ standard deviation for the dates of the 12 magnetic reversals from the top of the Kaena to the top of the Thvera is ± 18 ka (Lourens *et al*. 1996, table 3). Thus, precision of the order of a plus/minus one precession cycle is readily achieved among independent investigators. The veracity of the astronomically tuned GPTS has been independently verified by radiometric dating and the revisions are now widely accepted (Baksi *et al*. 1992, 1993; Hall & Farrell 1994; McDougall *et al*. 1992; Tauxe *et al*. 1992; Walter *et al*. 1991, 1992).

Another application of astronomical tuning is the stratigraphic correlation of globally distributed sites at the level sufficient to confidently evaluate lead and lag (phase) relationships among climate variables. This requires much smaller errors (optimally ± 2 or ± 3 ka) and is necessary in order to establish the climate response to external (insolation) forcing and to understand the physics underlying internal climate interactions. Such requirements have been met for the Pleistocene but require considerably more work for pre-Pleistocene sections.

During the Pleistocene, when the thermal inertia of the large Northern Hemisphere (NH) ice sheets sets the phase of the climate response, the phase of δ^{18}O relative to obliquity (tilt) and precession is reasonably well established; δ^{18}O minima lag NH summer insolation maxima by *ca*. 69° (7.8 ka) at the obliquity band and *ca*. 78° (5 ka) at the precession band (Imbrie *et al*. 1984). Thus, for Pleistocene sections, tuning δ^{18}O to insolation (with the appropriate phase lags) accomplishes two critical goals. First, because δ^{18}O is globally correlative, lead and lag (phase) relationships among climate variables from globally distributed sites can be accurately measured. Second, phase relationships between insolation forcing and climate response can be measured. These phase relationships are critical to the development of physical models of climate change on orbital time-scales (Imbrie *et al*. 1992, 1993). Such relationships are not well established for the pre-Pleistocene, a time during which the dominant terrestrial ice sheets shift from the Southern Hemisphere to the Northern Hemisphere and the phase of the climate response to insolation forcing may not be stationary (Clemens *et al*. 1996).

State-of-the-art tuning of Pliocene and older sections involves mapping cycles in variables such as dust content, carbonate content, magnetic susceptibility, colour reflectance, or gamma-ray attenuation porosity evaluator (GRAPE) directly to precession itself or to a precession-dominated insolation target with the assumption of a constant phase offset relative to insolation forcing. Unlike Pleistocene δ^{18}O these variables are not globally correlative and few have reliable models linking them to insolation forcing. This is an acknowledged deficiency of Pliocene astronomical tuning as indicated, for example, by Shackleton's statement regarding the phase of the GRAPE tuning parameter used for ODP (Ocean Drilling Program) Leg 138 sites (Shackleton *et al*. 1995*a*):

> In the case of GRAPE density (or the underlying variable, the ratio of calcite to biogenic opal), we do not have a model linking the forcing

> and the response. Therefore, we have simply used the calculated record of summer insolation at 65° N as the tuning target. We have throughout assumed that no phase lag existed between insolation and GRAPE density and that high density (high % $CaCO_3$) is associated with high Northern Hemisphere summer insolation. ... whether the same phase relationship is appropriate in the older part of the record, is not yet known.

A revised strategy for astronomical tuning within the Pliocene is presented in subsequent sections. The strategy ultimately relies on tuning the 41 ka component of δ^{18}O (δ^{18}O-41) to obliquity. The strategy is based on the assumption that, of all the available tuning parameters, δ^{18}O-41 is the most likely to be globally correlative and the least likely to be variable in phase relative to orbital forcing. This tuning strategy is applied to the 3–5 Ma intervals from ODP Site 659 (Tiedemann *et al.* 1994) and the Mediterranean *Rossello* (Vrica/Singa) Composite Section (Lourens *et al.* 1996) in an effort to assess its strengths and weaknesses.

2. Background

Most researchers have adopted a Pliocene strategy whereby the tuning parameter (e.g. sapropels, GRAPE, dust, colour reflectance, magnetic susceptibility, etc.) is mapped directly to orbital precession (P) or to an insolation target dominated by precession; usually summer insolation at 65° N (Clemens *et al.* 1996; Hilgen 1991*a*, *b*; Hilgen *et al.* 1993; Lourens *et al.* 1996; Shackleton *et al.* 1995*a*; Tiedemann & Franz 1998; Tiedemann *et al.* 1994). This approach has been adopted for two primary (and largely valid) reasons: (1) climate records are often dominated by precessional variance, especially in the low latitudes, and (2) precession modulates in easily recognized packets of *ca.* 100 and 400 ka cycles due to the influence of eccentricity. Thus, correlating 23 ka cycles in the tuning parameter to precession or to a precession-dominated insolation target is a relatively easy exercise provided the stratigraphic section is complete. This approach commonly assumes a constant phase relationship between the tuning parameter (GRAPE, dust, magnetic susceptibility, etc.) and orbital forcing. There are three primary reasons why this assumption may be unfounded.

First, precession insolation forcing is hemispherically asymmetric. That is, warm NH and Southern Hemisphere (SH) summers occur 180°, or 11.5 ka out of phase with one another at the precession band. In contrast, obliquity insolation forcing is hemispherically symmetric; warm summers occur in both hemispheres at the same time—there is no phase offset (figure 1). Second, the location of the dominant continental-scale ice sheets shifts from the SH to the NH over the course of the Pliocene. Combined, these facts lead to the possibility that the phase of δ^{18}O (as well as other climate parameters directly or indirectly related to changes in terrestrial ice volume) may shift by as much as 180° (*ca.* 11.5 ka) within the precession band. Third, commonly used tuning parameters (GRAPE, magnetic susceptibility, colour reflectance) respond to the combined influence of dilution by terrigenous material as well as carbonate and opal production and dissolution; processes which are strongly influenced by changes in global ice-volume and deep-ocean chemistry on both orbital and longer time-scales. Thus, there is no *a priori* reason to believe that the phase of these parameters should be invariant relative to precessional insolation forcing.

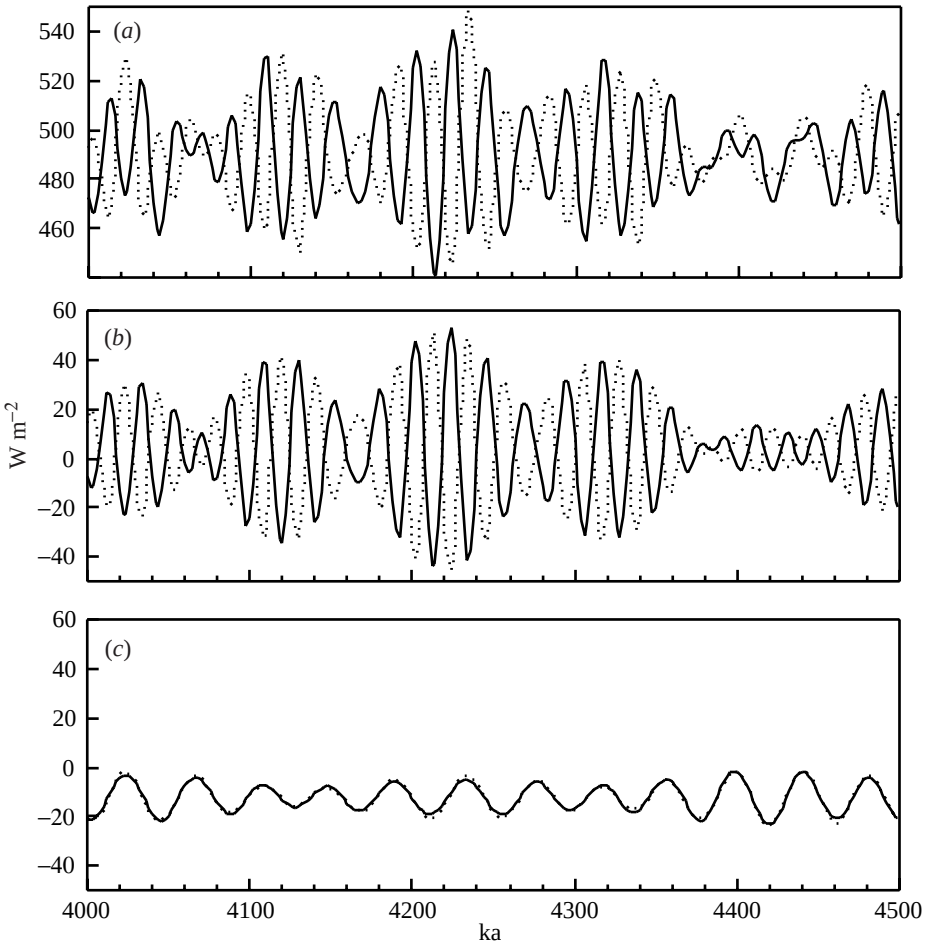

Figure 1. Phase relationships between Northern and Southern Hemisphere summer insolation forcing. (*a*) Summer insolation for December, 65° S (dashed line), and June, 65° N (solid line). (*b*) Precession bandpass filter of summer insolation for December, 65° S (dashed line), and June, 65° N (solid line). Summer insolation forcing for the Northern and Southern Hemispheres is 180° out of phase over the precession band. (*c*) Obliquity (tilt) bandpass filter of summer insolation for December, 65° S (dashed line), and June, 65° N (solid line). There is no phase offset within the obliquity band. The precession (23, 19 ka) bandpass filter uses 4 triangles, 138 filter weights, a central frequency of 0.04715 cycles ka^{-1}, a 2 ka time-step, and a bandwidth of 0.018 215 cycles ka^{-1}. The tilt (41 ka) bandpass filter uses 3 triangles, 118 filter weights, a central frequency of 0.02439 cycles ka^{-1}, a 2 ka time-step, and a bandwidth of 0.017 cycles ka^{-1}.

Tuning to 65° N insolation or directly to precession with a constant phase does not allow for the possibility of a time-varying phase response and can result in an astronomical time-scale that is off by up to 11.5 ka (180° in the precession band and by 101° in the obliquity band).

While an error of ±11.5 ka is small in an absolute sense, and has no impact on the accuracy of the GPTS, the corresponding uncertainty in phase precludes reliable interpretation of climate physics. Within the precession band, a 180° uncertainty precludes an understanding of which hemisphere, if either, is dominant. For example,

in the Pleistocene even SH climate records have precession-band phase responses linked directly to changes in NH ice volume (Imbrie *et al*. 1992, 1993). It is important to understand the extent to which dominance of SH ice volume in the Pliocene might similarly force aspects of the NH climate response. In terms of the obliquity response, the corresponding 101° uncertainty in phase precludes an evaluation of time constants internal to the climate system.

Clemens *et al*. (1996) document a clear example of phase drift within the precession band at Arabian Sea Site 722 (figure 2). The age model for Site 722 incorporates a 17 ka time constant for the ice-volume response to NH summer insolation. This is reflected in the near-constant phase of the glacial climate indices (δ^{18}O and dust) relative to summer insolation maxima. This age model suggests that the phase of the monsoon indices (lithogenic grain size and opal flux) drifts through time relative to insolation maxima. Alternatively, had the monsoon indices been tuned to NH summer insolation with a constant zero phase lag, they would plot along the 0° line, forcing the phase of δ^{18}O and dust flux to drift relative to insolation forcing. Clearly, both potential age models cannot be correct. In either case, however, the phase of the monsoon indices drifts significantly relative to dust flux and δ^{18}O. This result is independent of the age model as all indices were measured from the same core. These results clearly illustrate the potential problem of tuning in the precession band assuming a constant phase response relative to insolation forcing.

Based on these issues a rationale is presented for incorporating the obliquity component of δ^{18}O into the Pliocene astronomical tuning strategy. This procedure is then applied to the Site 659 and Mediterranean *Rossello* sediment sections in order to evaluate the viability of the approach. Note that neither Site 659 nor the *Rossello* records are optimal for this exercise. Site 659 may be missing section at core break 12/13 where overlapping cores required for construction of a composite were not recovered (Tiedemann *et al*. 1994). The Mediterranean is an isolated basin; as such the δ^{18}O signal may be influenced by local/regional temperature and salinity changes. Indeed, the precessional component of the Mediterranean δ^{18}O (δ^{18}O-23) is thought to reflect temperature and salinity variability associated with the changing environmental conditions of sapropel formation while δ^{18}O-41 is thought to reflect changes in global ice volume (Lourens *et al*. 1996). Nonetheless, these records are used in this exercise because they have associated climate variables (dust and δ^{18}O) which have strong precessional responses and reasonably constrained models linking them to insolation forcing.

3. Proposed tuning strategy incorporating δ^{18}O-41

Obliquity insolation forcing is symmetric in the NH and SH (figure 1). Provided that variability in δ^{18}O-41 is linked to high latitude processes, the phase of δ^{18}O-41 should not be significantly influenced by the SH to NH shift in the location of the dominant ice sheets during the Pliocene nor by changes in the location (SH versus NH) of predominant deep-water formation. Given this, the proposed precession/obliquity tuning (POT) strategy centres on the hypothesis that δ^{18}O-41 is the most likely climate variable to be globally correlative and the most stable in phase relative to orbital forcing regardless of whether it is driven by temperature, ice volume, or a combination thereof. On the other hand, variability in δ^{18}O-41 is very small in some intervals and thus difficult to tune whereas precession-band variance associated with

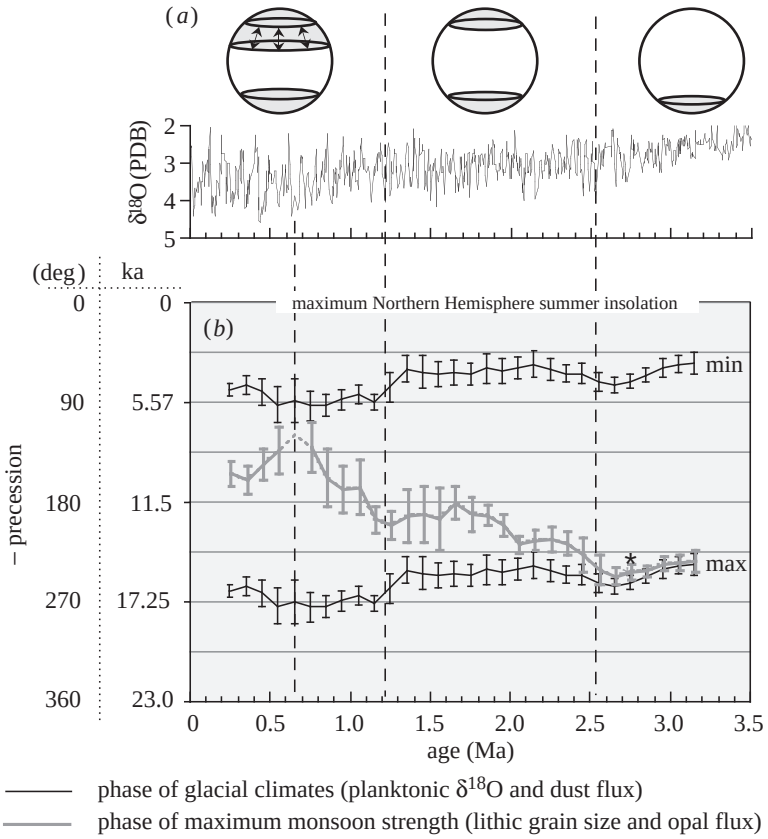

Figure 2. Plio-Pleistocene coherence and phase relationships among δ^{18}O, dust flux, monsoon strength, and orbital precession for Arabian Sea Site 722 (Clemens *et al*. 1996). (*a*) Marine δ^{18}O record (Tiedemann *et al*. 1994) and schematic evolution of Northern and Southern Hemisphere ice volume. Initial growth of significant NH ice sheets is recorded by three isotopically heavy events in δ^{18}O at *ca*. 2.6 Ma. Initiation of 100 ka ice-age cyclicity occurred at *ca*. 1.2 Ma. Amplification of the 100 ka cycle initiated at *ca*. 0.6 Ma. (*b*) The purpose of the phase plot is to display cross-spectral relationships among climate tracers and orbital insolation over the precession band. Each climate record is compared spectrally with the La90 orbital solution using a bandwidth of 0.008 887 ka^{-1} and a 500 ka window. The analysis window is stepped through the length of each record at 100 ka time-steps beginning at 0.25 Ma. The result of each analysis (and the associated error) is plotted at the midpoint of the 500 ka window provided statistical significance exceeds the 80% confidence interval (CI). Results where the CI is less than 80% are represented by a dashed line or are not plotted. Zero on the *y*-axis is set at maximum precession (−P; 21 June perihelion), coinciding with maximum NH summer radiation. The *y*-axis, 0° to −360°, represents one precession cycle (23 ka, 360°). Thus, each point, represented by an error bar, gives the phase of the maximum response of a climate variable relative to insolation forcing for a 500 ka interval of time. For example, the data point denoted by the asterisk (coordinates are −247°, 2.75 Ma) indicates that the monsoon maxima are coherent with orbital precession (CI more than 80%) and occur $-247 \pm 10°$ (15.8 ± 0.6 ka) after NH summer insolation maxima for the 500 ka interval from 3.0 to 2.5 Ma. For this plot, spectral results for lithogenic flux and δ^{18}O are combined as indices of glacial climates. Similarly, lithogenic grain size and opal flux are combined as indicators of monsoon strength. See Clemens *et al*. (1996) for details.

other variables is often quite robust and easy to tune. With these points in mind, the following strategy is proposed.

1. Tune an appropriate variable (dust, GRAPE, susceptibility, colour reflectance, etc.) to insolation or precession assuming a constant phase relationship (as is the currently accepted practice). As illustrated in the following sections, this often yields an excellent match between the geological data and orbital precession. This initial tuning, by association, should correlate 41 ka cycles in the δ^{18}O to the correct obliquity cycles even within intervals of muted δ^{18}O-41 variance.

2. Evaluate the phase of δ^{18}O-41 relative to obliquity. It should be constant. If not, adjust the age model to make it so. In effect, this relaxes the phase-lock to precession/insolation established in the first step. Any resulting phase drift in the climate response thus requires interpretation. As will be illustrated, this approach suggests the possibility that the phase response in the precession band may be variable within the 4–4.6 Ma intervals at Site 659 and the *Rossello* Section.

   Shackleton *et al*. (1995*a*) document that a long time constant exists in the Pliocene climate system, suggesting that a lag between δ^{18}O-41 and obliquity insolation forcing exists within the Pliocene insolation–ice system. For this work a 17 ka time constant is employed whereby δ^{18}O minima lag summer insolation maxima by *ca.* 7.8 ka at the obliquity band. However, the lag could be smaller (e.g. Lourens *et al*. 1996) and even change slightly through time with the evolution of Pliocene ice-volume. In any case, it is acknowledged that the time constant issue is underconstrained. For the purposes of this exercise, however, the choice of time constant is somewhat irrelevant; the phase drift described in the following sections will exist regardless of the time constant chosen.

4. Application to sediment records

(*a*) *Equatorial Atlantic Site 659*

The age model for Site 659 was developed by oxygen isotope correlation to Site 677 δ^{18}O (Shackleton *et al*. 1990) for the interval 0–2.85 Ma. In turn, Site 677 δ^{18}O was tuned to the Imbrie & Imbrie ice-volume model (Imbrie & Imbrie 1980). The Imbrie & Imbrie model incorporates a 7.8 ka phase lag between obliquity maxima and δ^{18}O-41 minima, consistent with a 17 ka time constant. For the interval 2.85–5 Ma, dust flux maxima were tuned to 65° N insolation minima using the Ber90 astronomical solution (Berger & Loutre 1991) assuming a constant zero phase offset (Tiedemann *et al*. 1994). This original age model is hereafter referred to as the T94 age model.

Over the interval 1–3 Ma, the T94 age model yields an excellent phase lock between δ^{18}O-41 and tilt prime (Tprm; obliquity with a 17 ka time constant) (figure 3*a*, *b*). This is consistent with having tuned Site 659 δ^{18}O to Site 677 δ^{18}O. Note, however, that the phase of dust-23 (the 23 ka bandpass filter of dust concentration) relative to precession is variable; it is *ca.* 180° out of phase over the interval 1.2–1.6 Ma (figure 3*c*).

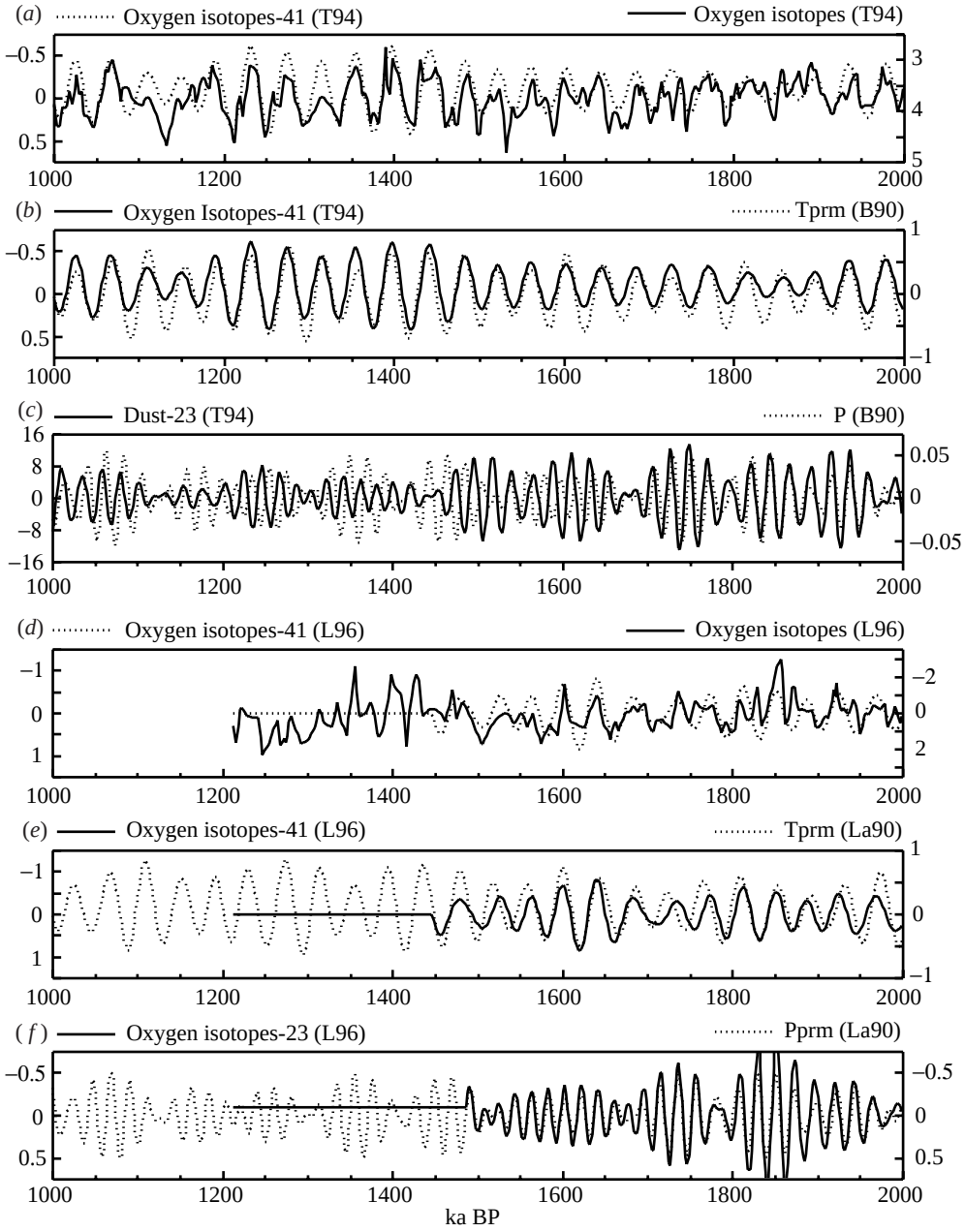

Figure 3. 41 and 23 ka bandpass filters of Site 659 (T94) and *Rossello* (L96) composite records (1–3 Ma) using the original age models. (*a*) 659 δ^{18}O and its 41 ka bandpass filter (δ^{18}O-41). (*b*) 659 δ^{18}O-41 and Tilt prime (Tprm). (*c*) 23 ka bandpass filter of 659 dust concentration (dust-23) and precession (P). (*d*) *Rossello* δ^{18}O and *Rossello* δ^{18}O-41. (*e*) *Rossello* δ^{18}O-41 and Tprm. (*f*) *Rossello* δ^{18}O-23 and precession prime (Pprm). Tprm (Pprm) is orbital obliquity (precession) passed through a single exponential system with a time constant of 17 ka. B90 is the Ber90 astronomical solution (Berger & Loutre 1991). La90 is the Laskar (1990) (0,1) astronomical solution (Laskar *et al*. 1993).

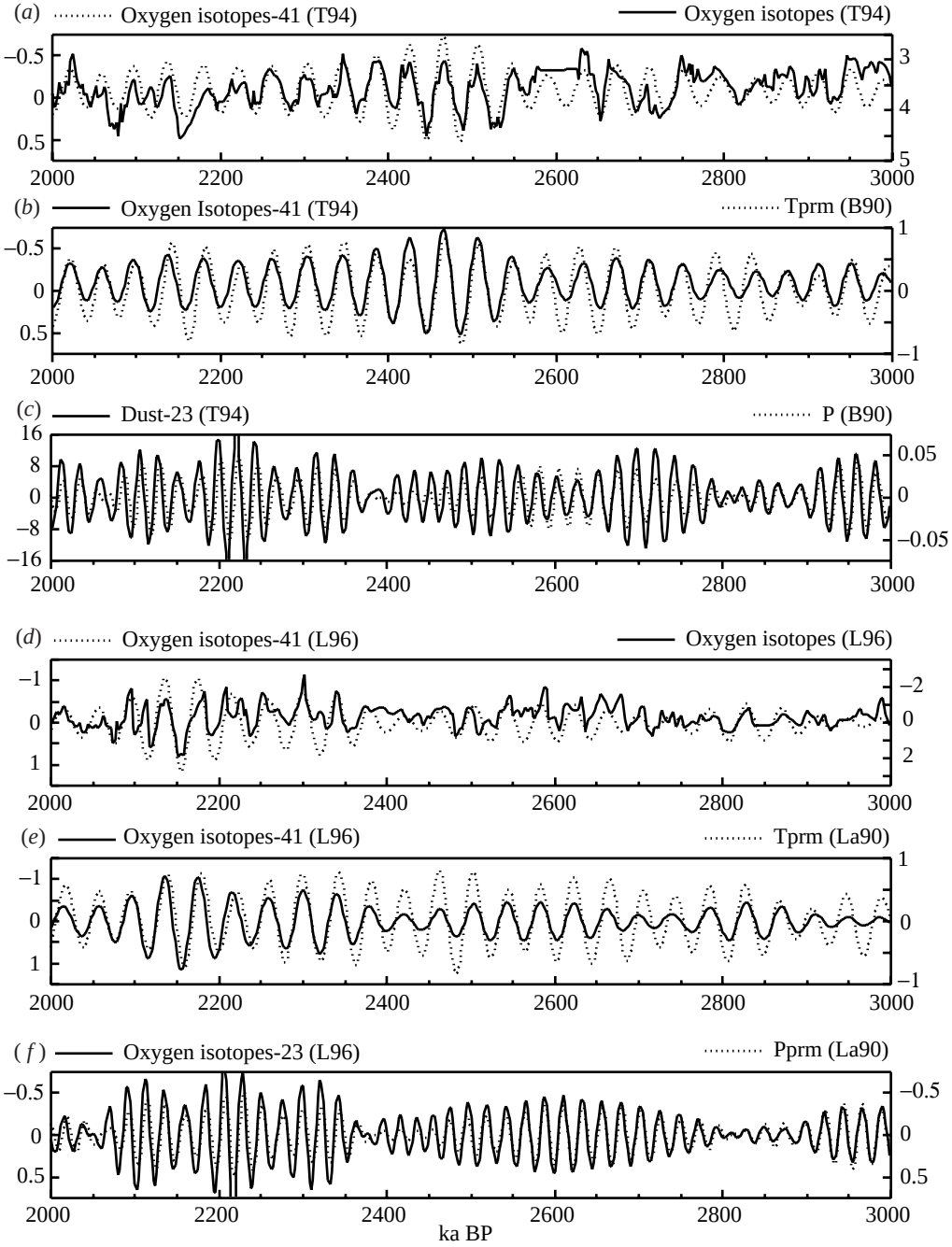

Figure 3. (*Cont.*)

On the other hand, over the interval 3–5 Ma, the T94 age model yields an excellent phase lock between dust-23 and orbital precession (P), consistent with having tuned dust to insolation (figure 4*a*). However, comparison between δ^{18}O-41 and Tprm indicates that the isotopic phase response is quite variable for this dust-tuned age model

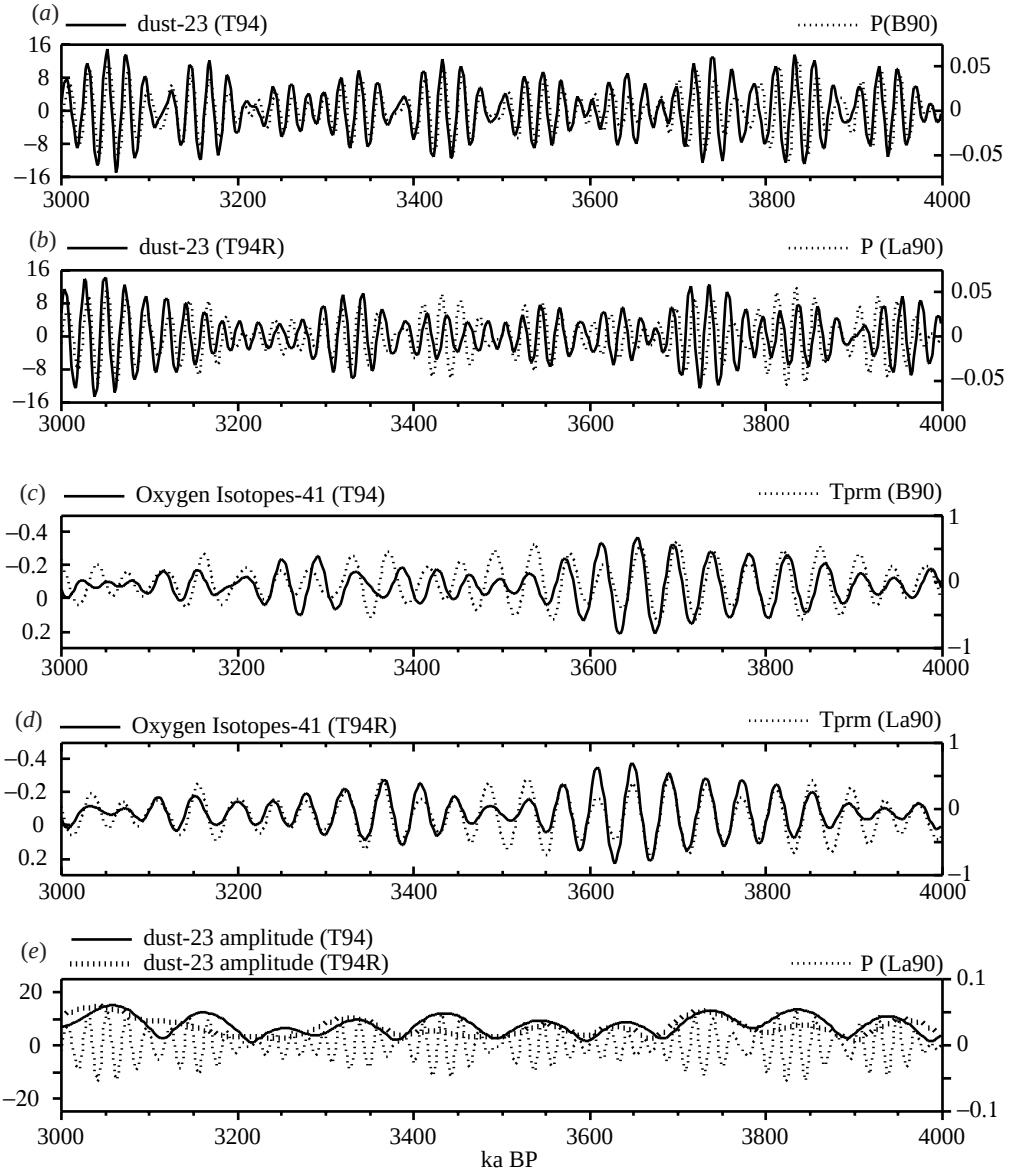

Figure 4. Bandpass filter and amplitude modulation of Site 659 dust concentration and δ^{18}O records (3–5 Ma) comparing the original (T94) and revised (T94R) age models. T94 was developed by tuning dust maxima to 65° N insolation minima using the B90 astronomical solution (Berger & Loutre 1991). T94R builds on T94 by further tuning depleted δ^{18}O-41 to Tprm using the La90(0,1) astronomical solution. (*a*) Site 659 dust-23 (T94 age model) compared with precession. (*b*) Site 659 dust-23 (T94R age model) compared with precession. (*c*) Site 659 δ^{18}O-41 (T94 age model) compared with Tprm. (*d*) Site 659 δ^{18}O-41 (T94R age model) compared with Tprm. (*e*) Amplitude of the dust record on both the T94 and T94R age models compared with precession. For the purposes of examining amplitude modulation B90 and La90 are comparable, either could be used here. The amplitude modulation is calculated from Hilbert transform (Barnett 1983) of the bandpass filters.

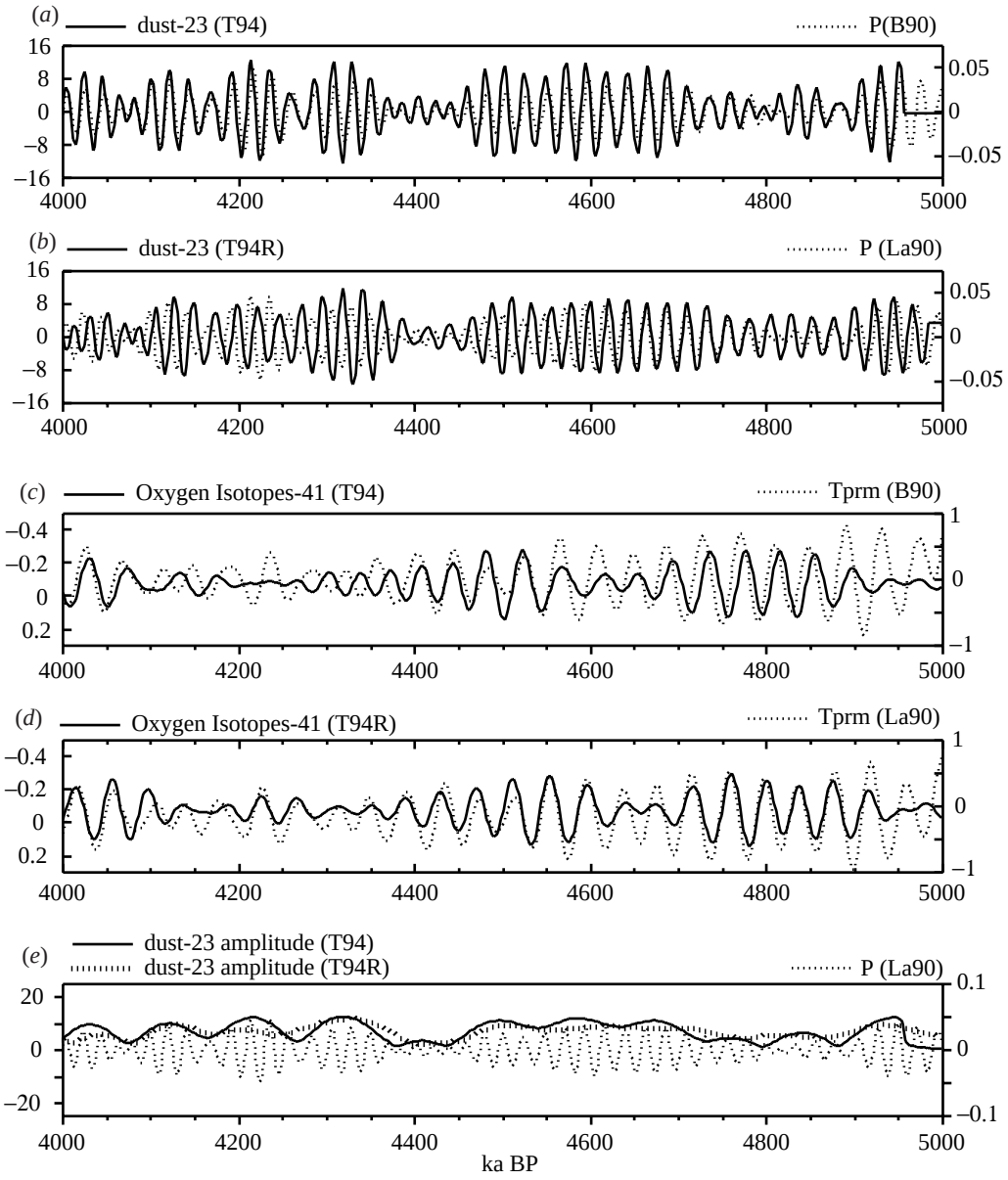

Figure 4. (*Cont.*)

(figure 4*c*); sometimes leading (e.g. 4.8–4.6 Ma), sometimes in phase (e.g. 4–3.6 Ma) and sometimes out of phase (e.g. 4.4–4.1 Ma). Thus, relative to the 1–3 Ma interval, the phase relationship between δ^{18}O-41 and Tprm is significantly degraded over the interval 3–5 Ma where the T94 tuning strategy shifts from mapping δ^{18}O-41 to Tprm to mapping dust to insolation.

Following the proposed tuning strategy, a revised age model (T94R) is developed for the interval 3–5 Ma in which δ^{18}O-41 is tuned to Tprm. For this tuning the Laskar (1990) (0,1) orbital solution (hereafter La90) is used as a target since it is now widely

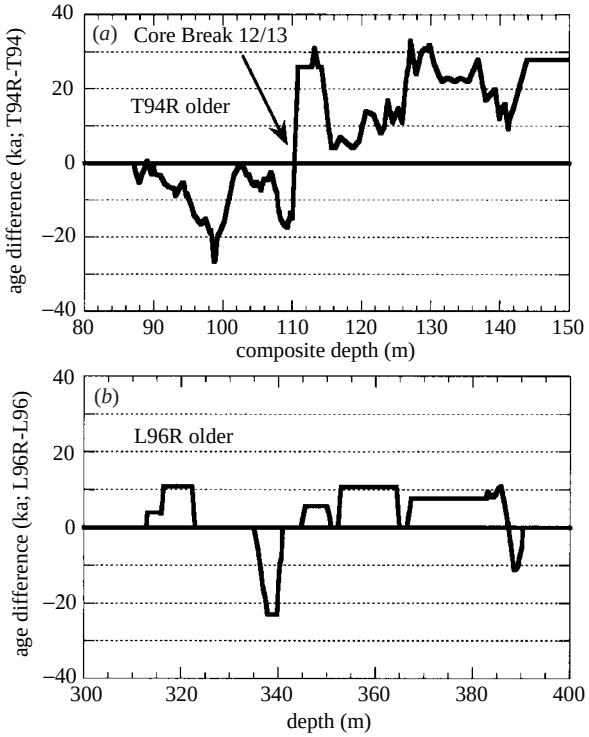

Figure 5. Age differences between the original and revised age models for (*a*) Site 659 and (*b*) the *Rossello* Composite Sections over the 3–5 Ma interval.

accepted as more appropriate than the B90 solution (Laskar 1990; Laskar *et al*. 1993; Lourens *et al*. 1996). While Lourens *et al*. (1996) prefer the La90 (1,1) solution, it makes little difference, for the purposes of this exercise, which version of the La90 solution is used.

The most significant difference between the T94 and T94R age models is the addition of a 41 ka cycle at core break 12/13 at *ca*. 3.9 Ma (figure 5). The revised age model (T94R) yields an improved phase and amplitude match between δ^{18}O-41 and Tprm (figure 4*c*, *d*). On the other hand, it yields a somewhat degraded amplitude match between dust-23 and precession (figure 4*e*). Of primary relevance to this exercise, the T94 age model removes the phase lock between dust-23 and precession. The result is that dust-23 is out of phase with precession over the interval 4.6–4 Ma (figure 4*b*). The significance of the drift within this interval is somewhat uncertain, especially from 4.4 to 4.1 Ma where the δ^{18}O record has little 41 ka variance and a small-amplitude response (figure 6*a*) which makes tuning difficult within the obliquity band. However, it is important to recall that a similar out-of-phase response also occurs in the interval 1.6–1.2 Ma where the δ^{18}O-41 variance is strong and easily tuned (figure 3*a*–*c*).

(*b*) *Mediterranean Rossello Composite Section*

The age model for the lower Pliocene *Rossello* Composite Section from southern Sicily is based on tuning sedimentary carbonate (sapropel) cycles to NH summer

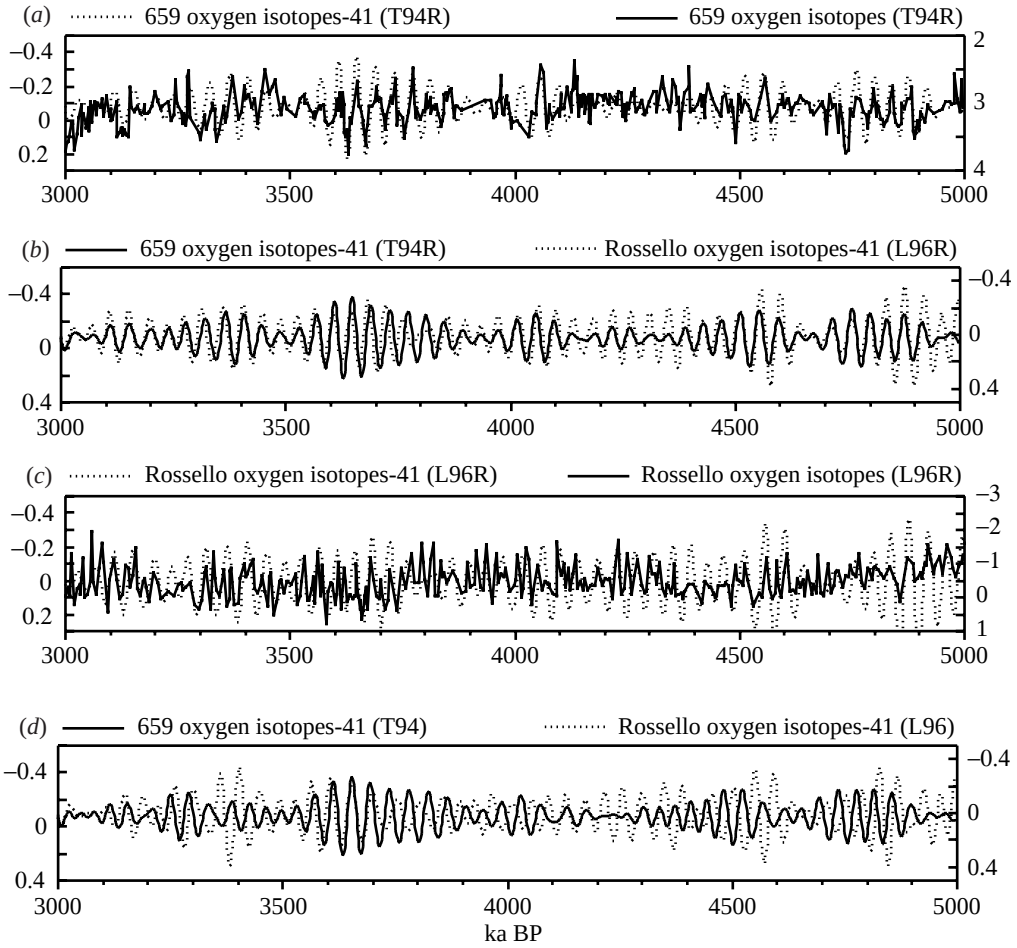

Figure 6. Comparison of δ^{18}O and δ^{18}O-41 for Site 659 and *Rossello*. (*a*) 659 δ^{18}O and δ^{18}O-41 on the revised (T94R) age model. (*b*) 659 δ^{18}O-41 and *Rossello* δ^{18}O-41 on the revised age models (T94R and L96R). (*c*) *Rossello* δ^{18}O and δ^{18}O-41 on the revised (L96R) age model. (*d*) 659 δ^{18}O-41 and *Rossello* δ^{18}O-41 on the original precession-tuned age models (T94 and L96). Comparison of (*b*) and (*d*) shows that the revised (precession/obliquity-tuned) age models yield a good amplitude correspondence between the two δ^{18}O-41 records. The original precession-tuned age models do not.

insolation (June and July averaged at 65° N) using the L90(1,1) solution (Laskar *et al*. 1993; Lourens *et al*. 1996). To be specific, the midpoints of low carbonate grey marl beds are correlated to insolation maxima (precession minima) with a constant 3 ka lag imposed throughout the Pliocene section. The 3 ka lag is based on the difference between the calendar age of the youngest Holocene sapropel (S-1) (radiocarbon dated at 8.5 ka) and the correlative 65° N summer insolation maximum (11.5 ka). This original age model is hereafter referred to as the Lourens *et al*. (1996) (L96) age model.

Similar to the Site 659 dust record, the *Rossello* planktonic δ^{18}O record has an exceptional precession signal. The L96 age model yields an excellent amplitude match

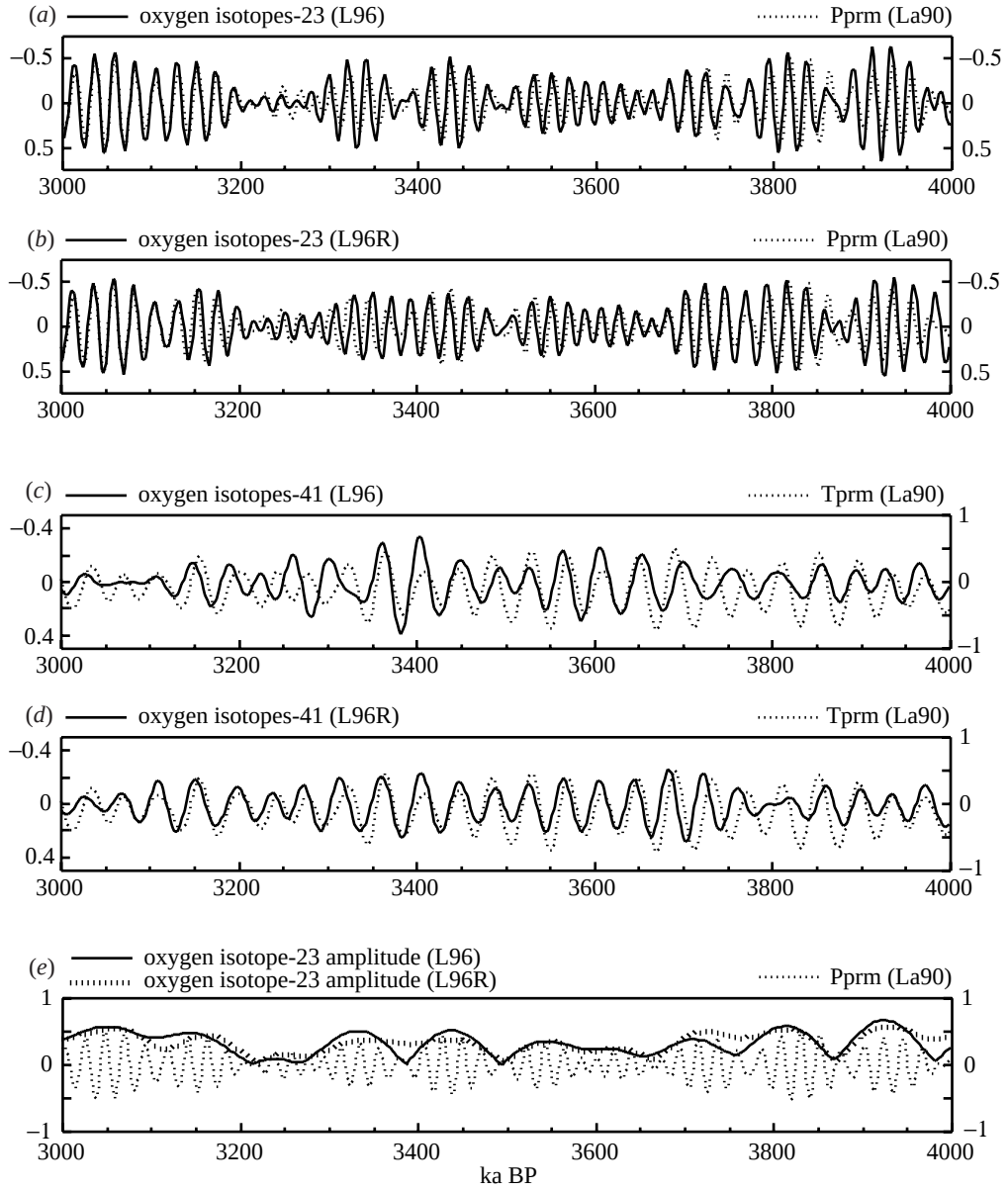

Figure 7. Bandpass filter and amplitude modulation of the *Rossello* δ^{18}O records (3–5 Ma) comparing the original (L96) and revised (L96R) age models. L96 was developed by tuning sedimentary carbonate cycles to NH summer insolation (June and July averaged at 65° N) using the L90(1,1) solution. L96R builds on L96 by further tuning depleted δ^{18}O-41 to Tprm using the La90(0,1) astronomical solution. (*a*) *Rossello* δ^{18}O-23 (L96 age model) compared with Pprm. (*b*) *Rossello* δ^{18}O-23 (L96R age model) compared with Pprm. (*c*) *Rossello* δ^{18}O-41 (L96 age model) compared with Tprm. (*d*) *Rossello* δ^{18}O-41 (L96R age model) compared with Tprm. (*e*) Amplitude of the δ^{18}O-23 records on both the L96 and L96R age models compared with Pprm. Amplitude modulation is calculated from the Hilbert transform (Barnett 1983) of the bandpass filters.

PHILOSOPHICAL TRANSACTIONS OF THE ROYAL SOCIETY A MATHEMATICAL, PHYSICAL & ENGINEERING SCIENCES

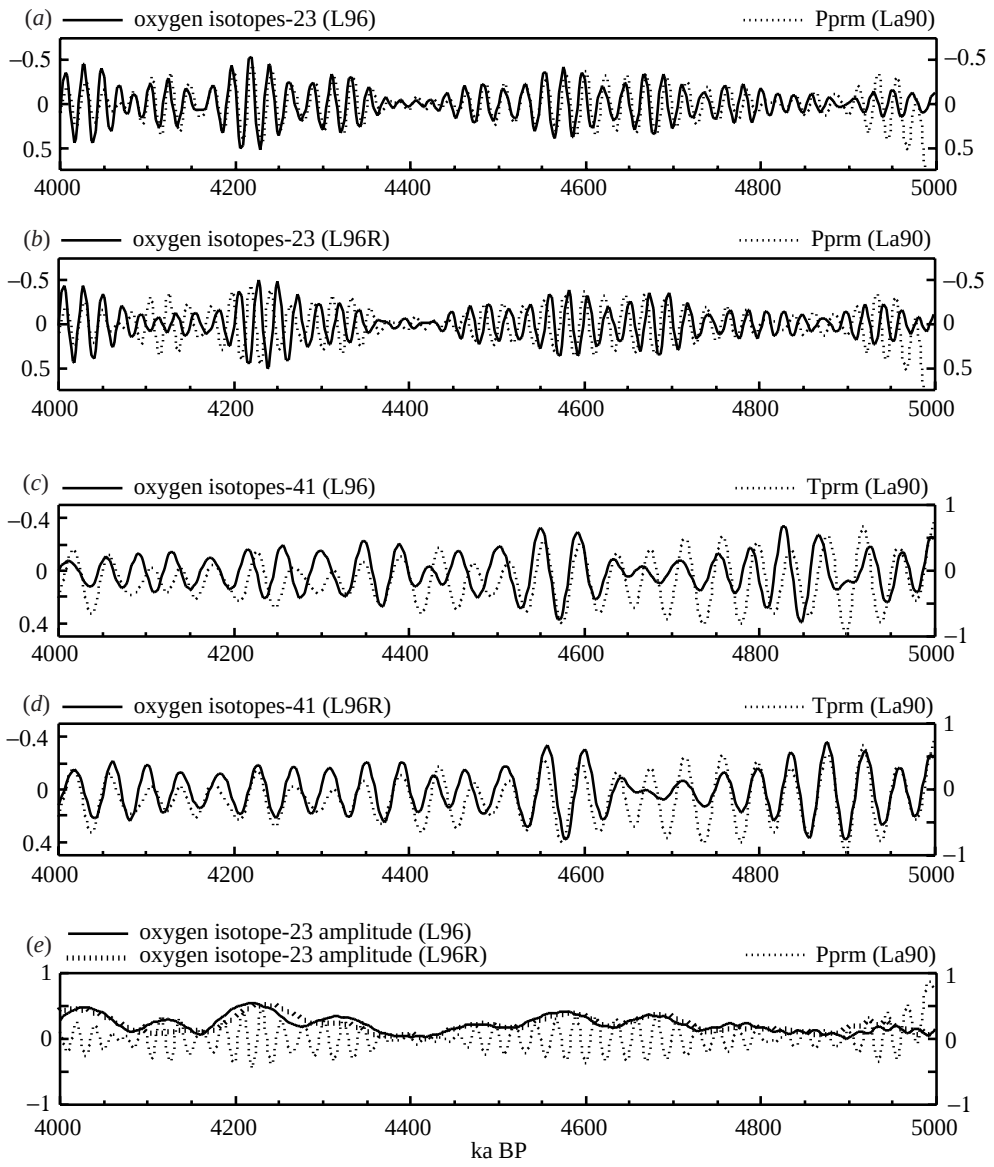

Figure 7. (*Cont.*)

and phase lock between the 23 ka component of δ^{18}O (δ^{18}O-23) and Pprm (precession with a 17 ka time constant) (figure 7*a*, *e*). However, on this precession-tuned age model the phase of δ^{18}O-41 relative to Tprm is quite variable (figure 7*c*). A small portion of this mismatch is due to the difference between the La90(1,1) tuning target used in the L96 age model and the La90(1,0) solution used in this paper. However, the difference between the two astronomical solutions is relatively constant (*ca.* 3 ka) over the interval 3–5 Ma whereas the differences between Tprm and δ^{18}O-41 range from 0 to 20 ka. Thus, the use of the two different solutions is of little consequence to the overall results of this exercise.

Following the proposed tuning strategy, a revised age model (L96R) is developed in which δ^{18}O-41 is tuned to Tprm. The revised age model (L96R) yields an improved overall match between δ^{18}O-41 and Tprm (figure 7*c*, *d*). With one exception, the age model adjustments are of the order of ±11 ka (figure 5). For the interval 3.77–3.67 the L96R ages are *ca.* 23 ka younger; this change improves the amplitude match between δ^{18}O-41 and Tprm within this interval. However, examination of the phase plot (figure 7*d*, *ca.* 3.7 Ma) suggests that the match to Tprm could be improved, making the 23 ka age difference smaller within this interval. Similar to the Site 659 results, the L96R age model yields a slightly degraded amplitude match between δ^{18}O-23 and Pprm relative to the L96 age model (figure 7*e*). The primary difference is that phase of δ^{18}O-23 is allowed to drift. The result is that δ^{18}O-23 is out of phase over the interval 4.4–4.1 Ma (figure 7*b*). This is similar to the drift found within the interval 4.6–4.0 Ma at Site 659. *Rossello* δ^{18}O has marginally better 41 ka structure within this interval relative to 659 (figure 6*a*, *c*) and the match to Tprm is somewhat better (figure 7*d*). However, given the overall marginal δ^{18}O-41 variability, the significance of the phase drift in this interval remains in question.

(*c*) *Age model evaluation*

As pointed out by Shackleton *et al*. (1995*b*) complex demodulation is more appropriate than cross-spectral analysis for comparing the amplitude modulation of a climate record with that of a proposed forcing mechanism while spectral and cross-spectral analysis is more appropriate for assessing phase relationships and the relative concentrations of variance at orbital periods. The revised age models for the Site 659 and *Rossello* records yield somewhat degraded amplitude matches with precession (figures 4*e* and 7*e*). However, the revised age models result in significantly increased concentrations of variance in δ^{18}O-41 for the *Rossello* Section, significantly increased coherence between *Rossello* δ^{18}O-41 and Site 659 δ^{18}O-41, and increased coherence between Site 659 dust and orbital parameters at both the eccentricity and tilt bands.

The T94R age model results in significantly increased coherence with eccentricity and obliquity for both dust (figure 8*a*, *b*) and δ^{18}O (figure 8*c*, *d*). However, coherence at the 23 and 19 ka bands is dramatically decreased for both. This results directly from phase drift within the precession band. Averaged over the interval 3–5 Ma, phase drift causes coherence to decrease below significant levels. However, analysis over short intervals where phase drift is small indicates coherence well above the 80% confidence interval (CI).

The revised age model for the *Rossello* record (L96R) yields a 60% increase in δ^{18}O variance at the obliquity band (figure 8*e*, *f*). As with Site 659, coherence with precession is much reduced when averaged over the 3–5 Ma interval but very strong when analysed over shorter intervals of time marked by smaller phase drift.

A primary rationale for tuning δ^{18}O to Tprm is the hypothesis that δ^{18}O-41 is the most likely variable to be globally correlative. If so, one expects coherence between δ^{18}O-41 from Site 659 and the *Rossello* Section. The original, precession-tuned age models, show no coherence between the two δ^{18}O-41 records at the obliquity band (figure 9*a*). The revised age models show coherence well above the 95% CI at the obliquity band with coherence above the 95% CI at the precession band as well (figure 9*b*). Note that the low coherence in figure 9*a* is not related to the difference in astronomical solutions (B90 versus La90). Cross-spectral analysis of these two

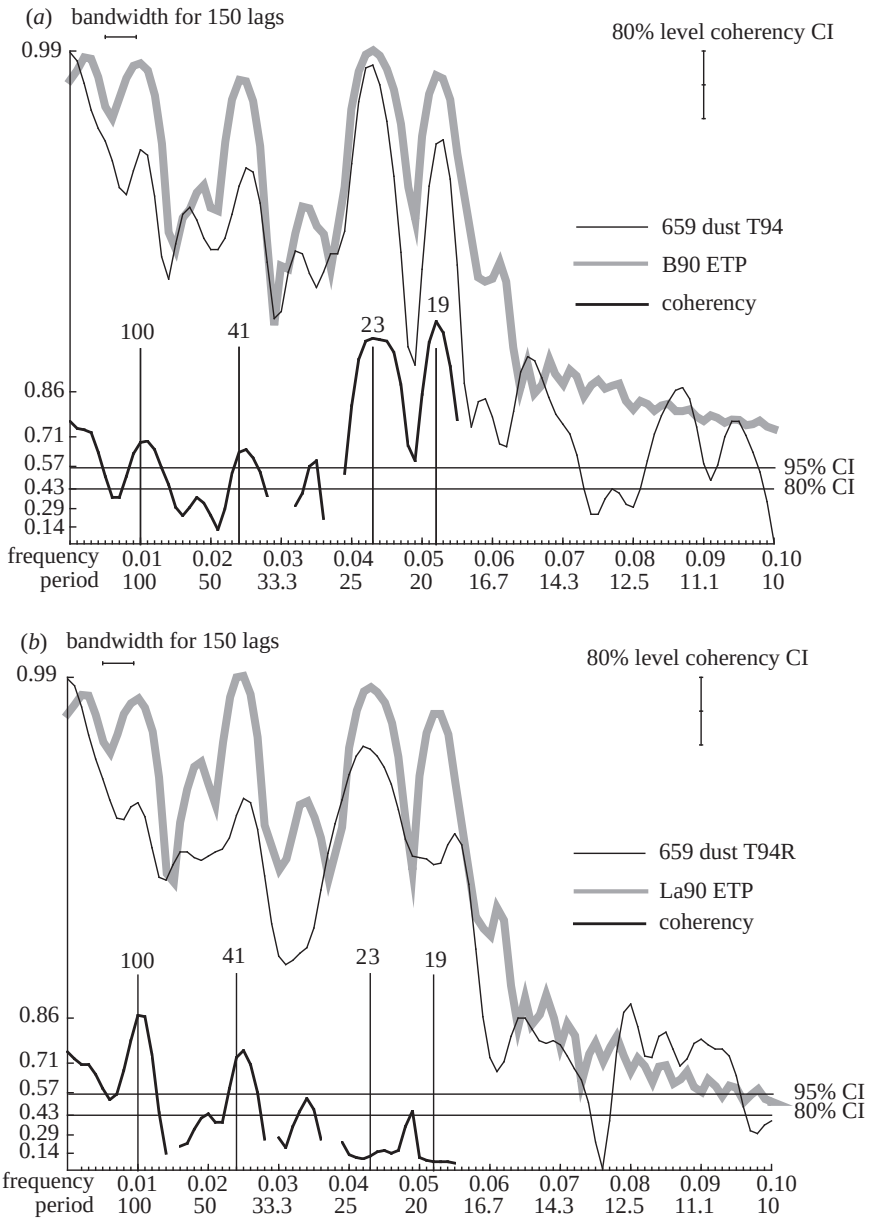

Figure 8. Cross-spectral analyses for Site 659 and *Rossello* records (3–5 Ma). (*a*), (*b*) 659 dust and ETP for the T94 and T94R age models. ETP is a record of normalized and averaged eccentricity (E), obliquity (tilt; T) and precession (P). Non-zero coherency at the 80% and 95% confidence intervals (CI) are indicated by solid horizontal lines.

solutions over the interval 3–5 Ma show coherence well above the 95% CI at all orbital periods (figure 10).

Another means of assessing results of the revised age models is by comparing the amplitude modulation of the two δ^{18}O-41 signals. With the exception of the interval from 4.4 to 4.1 Ma, the *Rossello* and Site 659 records have very similar δ^{18}O-

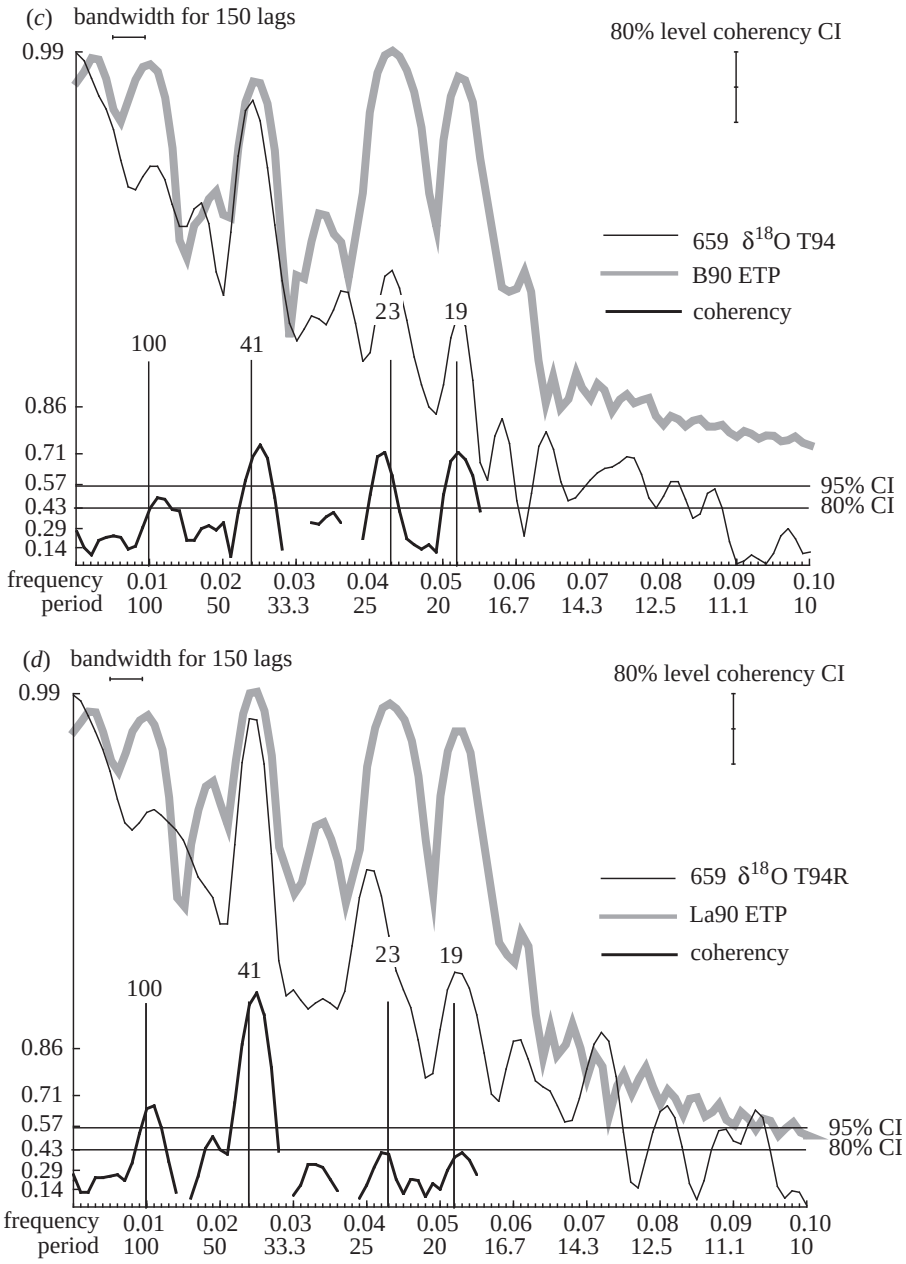

Figure 8. (*Cont.*) (*c*), (*d*) 659 δ^{18}O and ETP for the T94 and T94R age models.

41 amplitude modulation (figure 6*b*), indicating that they share common forcing within the obliquity band. This is further supported by the fact that the δ^{18}O-41 variability is similar in both records (*ca.* 0.35‰), whereas the δ^{18}O variability in the *Rossello* record (*ca.* 1.3‰) is twice that in the Site 659 record (*ca.* 0.6‰). Given that the comparison is between a planktonic record from the Mediterranean and a benthic record from the deep Atlantic, similar δ^{18}O-41 variability in overall

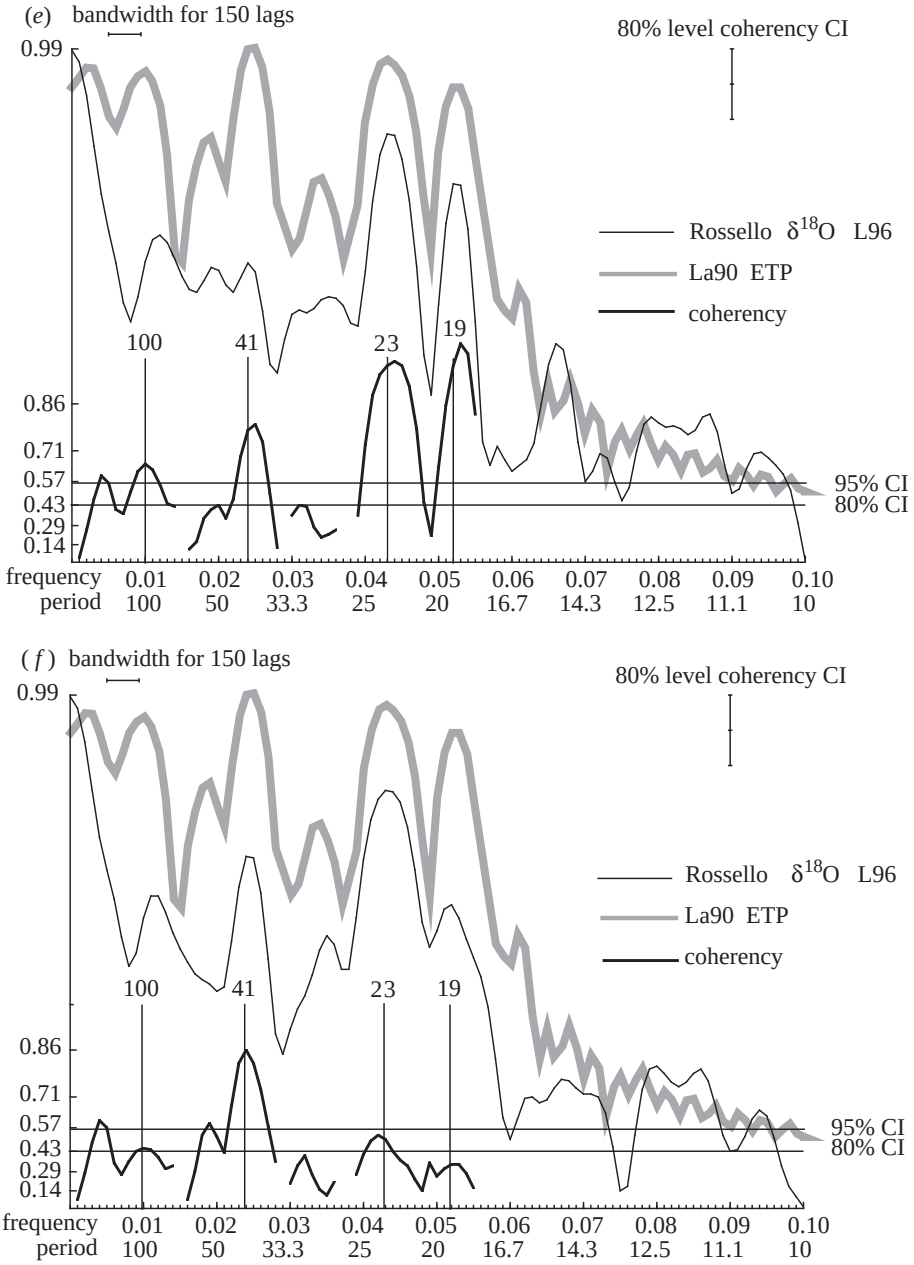

Figure 8. (*Cont.*) (*e*), (*f*) *Rossello* δ^{18}O and ETP for the L96 and L96R age models.

amplitude and amplitude modulation indicates that the common forcing is related primarily to changes in ice volume. Applying the Fairbanks & Matthews (1978) sea-level calibration (0.011‰ m^{-1}) to the 0.35‰ δ^{18}O-41 variability suggests a sea-level range of the order of 30 m in the interval 5–3 Ma. This signal should be common to all marine δ^{18}O records, thus providing a basis for global-scale correlation among Pliocene sections.

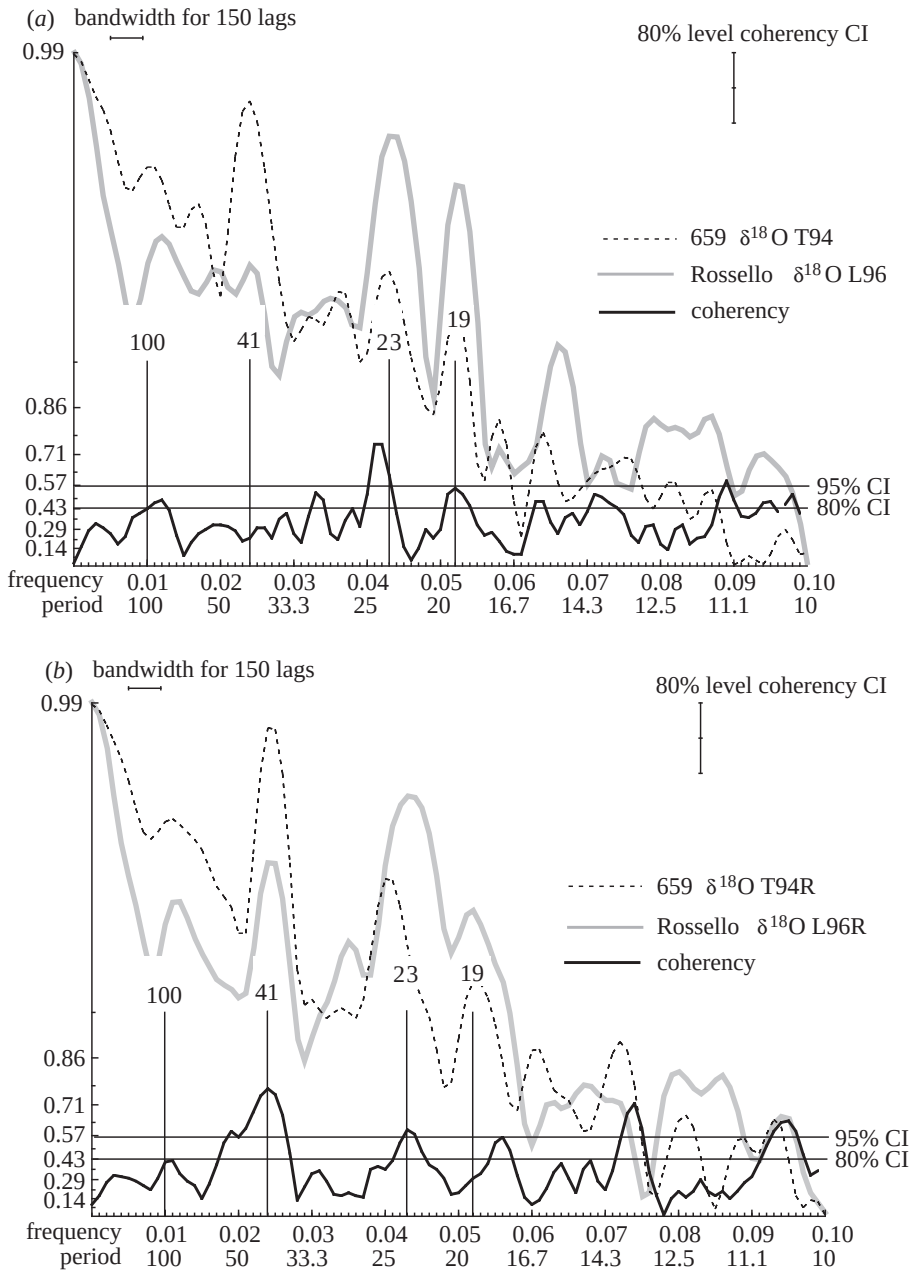

Figure 9. Cross-spectral comparison of Site 659 and *Rossello* δ^{18}O records on the original and revised age models (3–5 Ma). (*a*) Comparison using the precession-tuned T94 and L96 age models. Note coherence only at the precession band. (*b*) Comparison using the precession and obliquity-tuned T94R and L96R age models. Note coherence at the obliquity and precession bands. Non-zero coherency at the 80% and 95% confidence intervals (CI) are indicated by solid horizontal lines.

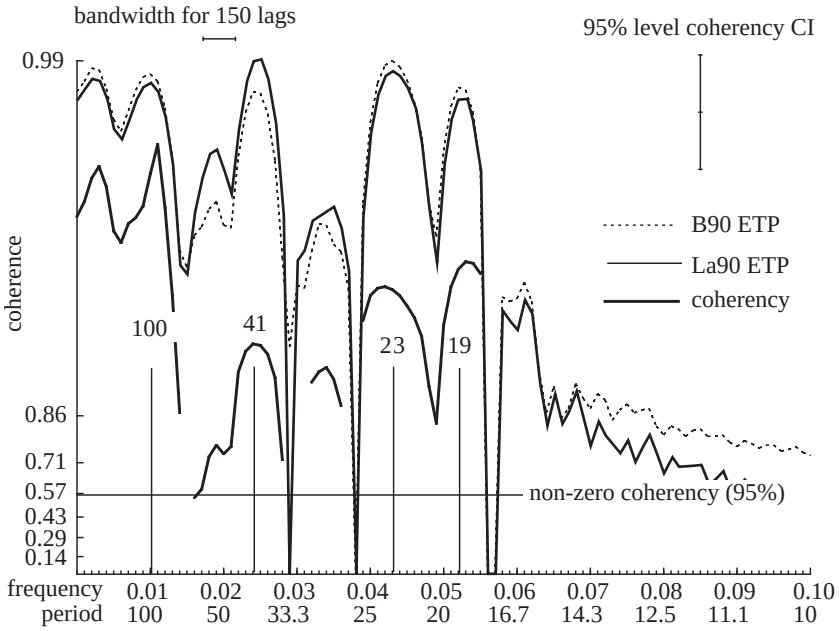

Figure 10. Cross-spectral comparison of ETP using the B90 and L90 astronomical solutions over the interval 3–5 Ma. Note strong coherence across all orbital periods.

5. Further research

Increased concentrations of variance in δ^{18}O-41 for the *Rossello* Section, increased and strong coherence between δ^{18}O-41 from the 659 and *Rossello* Sections, and similar δ^{18}O-41 amplitude modulation all support incorporating δ^{18}O-41 into the astronomical tuning strategy. However, the results presented here, from only two sites, are insufficient to confidently state that the POT strategy should replace the precession-based tuning strategy or that the revised age models should replace the published Site 659 and *Rossello* age models at this point. Confirmation of the proposed strategy will require application of the revised tuning strategy to other Pliocene records with attention to the following questions and issues.

(*a*) *Is* δ^{18}O-41 *globally correlative?*

Success of the proposed tuning strategy hinges on the correlative nature of δ^{18}O-41 and its utility as a tool for chronostratigraphic correlation within the Pliocene. Results from this work indicate similar amplitude modulation and high coherence between the Site 659 and the Mediterranean δ^{18}O-41 (with the exception of the interval from 4.4 to 4.1 Ma). This is encouraging given the distinct nature of the two records; *Rossello* δ^{18}O is a planktonic record derived from uplifted sections within the Mediterranean while Site 659 is a benthic record from the deep Atlantic. Comparison with additional Pliocene records from the Indian and the Pacific are required either to confirm the utility Pliocene δ^{18}O-41 as a reliable stratigraphic tool or to demonstrate that the degree of correlation achieved in this exercise is an artefact of overtuning.

(*b*) *Stationary and non-stationary phase relationships*

Clemens *et al*. (1996) document that the phase of strong monsoons has drifted relative to glacial maxima (δ^{18}O and dust flux) by *ca*. 83° in the precession band and *ca*. 124° in the obliquity band. Changes in the rate of phase drift coincide with key times in the growth of ice volume (at 2.6, 1.2 and 0.6 Ma), implicating the evolution of ice volume as a factor in driving the non-stationary response. These results suggest (a) that the monsoon and/or the ice-volume response is not stationary in phase relative to insolation forcing, and (b) that climate variables from other sites may also be non-stationary in phase relative to δ^{18}O and/or insolation forcing.

By phase-locking GRAPE, magnetic susceptibility, carbonate cycles, and dust cycles to precession, the precession-based tuning approach automatically forces any and all phase drift onto the δ^{18}O record. Whether or not this is valid can be evaluated by employing the POT approach to a set of globally distributed sites and assessing the coherence and amplitude modulation of the associated δ^{18}O-41 records as well as the coherence and phase relationships of the associated climate variables. Take, for example, the intervals where Site 659 dust-23 appears to drift (4.6–4.0 and 1.6–1.2 Ma). Dust concentration at Site 659 is estimated by measuring carbonate (100 minus wt% $CaCO_3$) and assuming a two-component sedimentary system. If similar phase drift is observed in carbonate-based indices from other sites (e.g. GRAPE and magnetic susceptibility), then one might evaluate changes in the phase and intensity of carbonate dissolution as a means of explaining phase drift within these two intervals (figure 11).

(*c*) *The climatic phase response relative to orbital forcing*

A better understanding of the phase relationships among climate variables and the mechanisms behind observed phase drift should provide a means of evaluating the phase of the climate response relative to insolation forcing. Continuing with the hypothetical dust example, an enhanced understanding of how changes in the intensity and timing of carbonate dissolution might impact on the phase of the observed dust signal would allow deconvolution of the signal into its 'dissolution' and 'atmospheric' components as illustrated schematically in figure 11. The atmospheric component may prove to be stationary in phase relative to precessional insolation forcing, consistent with the Tiedemann *et al*. (1994) model relating dust generation to monsoon intensity and insolation forcing. A stable phase response for both the atmospheric component of dust-23 and δ^{18}O-41 relative to insolation forcing, with plausible physical models for each, is the type of independent evidence needed to reliably estimate the climatic phase response to insolation forcing during the Pliocene.

6. Summary

The two astronomical tuning strategies evaluated in this work have fundamentally different underlying assumptions. Implicit in the precession-based tuning approach is the hypothesis that all variables with strong 23 ka cyclicities are phase locked to one another and to insolation forcing throughout the Pliocene. Taken to its extreme, this suggests that records of colour reflectance from the central Pacific, magnetic susceptibility from the equatorial Atlantic, dust from Africa, and carbonate cycles (sapropels) from the Mediterranean are all highly coherent and phase locked both

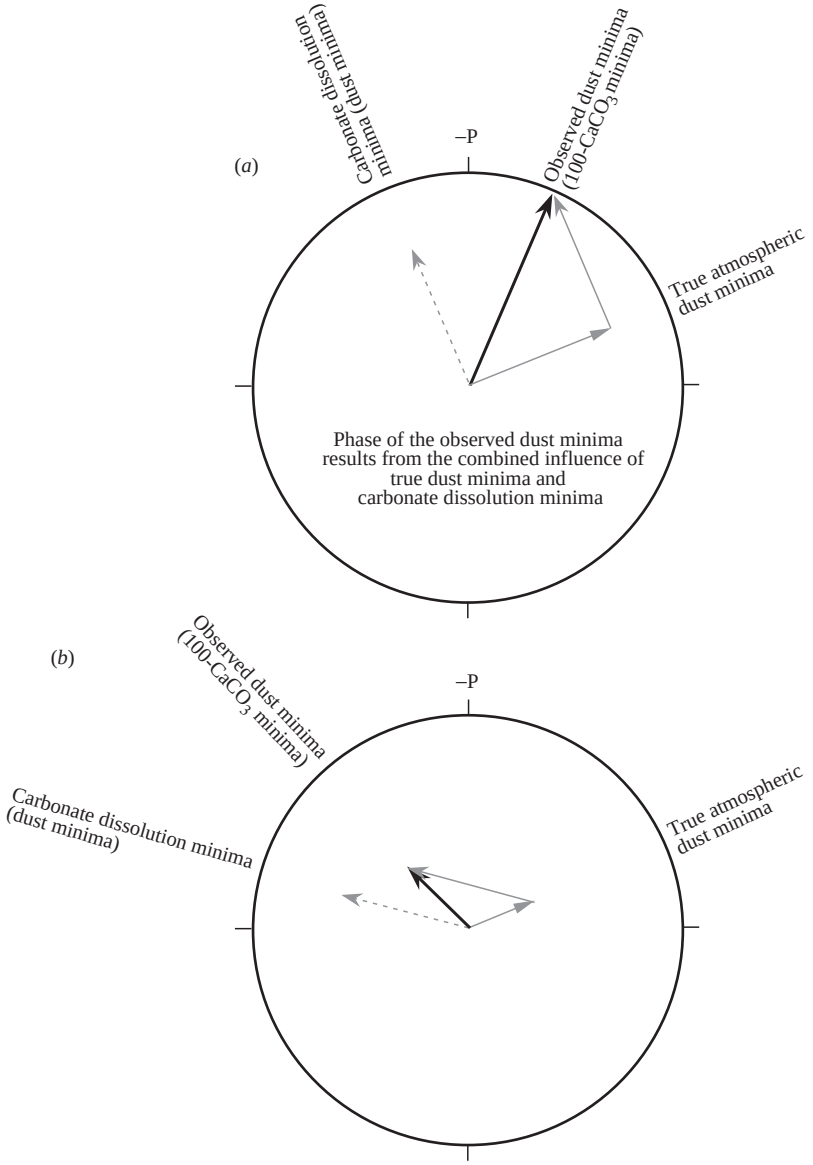

Figure 11. Vector addition cartoon illustrating how the observed phase response of dust concentration might result from atmospheric input of dust as well as $CaCO_3$ dissolution. The length of each vector represents the relative strength of the process. The observed response (black vector) is the sum of the labelled atmospheric (grey) and dissolution (dashed) vectors. The dashed dissolution vector is replicated as a grey vector and added to the atmospheric vector. The phase of the observed minima in example (*b*) is different from that in (*a*) due to a phase shift in the dissolution forcing and a decrease in the strength of the atmospheric input. The same concept applies equally to magnetic susceptibility (where the magnetic component is derived from fluvial or atmospheric processes) and GRAPE density or colour reflectance (where density and colour differences stem from relative concentrations of biogenic carbonate, opal, and terrigenous material). Note that this figure is an illustrative cartoon; it is not based on actual data from Site 659.

with one another and with insolation forcing while the phase relationships among their respective δ^{18}O records vary widely. Given the correlative nature of marine δ^{18}O, this seems unlikely.

The POT strategy takes the opposite approach; it is based on the assumption that δ^{18}O-41 is the variable most likely to be globally correlative and least likely to drift widely in phase relative to insolation forcing. The former is testable by examination of coherence and amplitude modulation relationships among δ^{18}O-41 records from globally distributed sites. The latter is considerably more difficult to test. However, if δ^{18}O-41 proves to be correlative, tuning within the obliquity band will allow further evaluation of phase relationships within the precession band and thus the development of more reliable models linking the response of specific climate variables (monsoon indices, dust generation, upwelling, etc.) both to one another and to insolation forcing. This, in turn will feed back into more reliable estimates of the δ^{18}O phase response relative to insolation forcing.

I thank John Imbrie and Angeline Duffy for extensive discussions of the issues and strategies involved in astronomical tuning. Thanks to Sir Nicholas Shackleton, Nick McCave and Graham Weedon for convening the Royal Society Discussion Meeting where these issues and strategies could be presented, debated and discussed, and to Lucas Lourens and Ralf Tiedemann for making available the excellent data-sets used in this work. This manuscript benefited from a review kindly provided by Lucas Lourens. This work was supported by the National Science Foundation grant OCE-971412.

References

Baksi, A. K., Hsu, V., McWilliams, M. O. & Farrar, E. 1992 ^{40}Ar/^{39}Ar dating of the Brunhes/Matuyama geomagnetic field reversal. *Science* **256**, 356–358.

Baksi, A. K., Hoffman, K. A. & McWilliams, M. 1993 Testing the accuracy of the geomagnetic time-scale (GPTS) at 2–5 Ma, utilizing ^{40}Ar/^{39}Ar incremental heating data on whole-rock basalts. *Earth Planet. Sci. Lett.* **118**, 135–144.

Barnett, T. P. 1983 Interaction of the monsoon and Pacific trade wind system at interannual time scales. Part I. The equatorial zone. *Mon. Weather Rev.* **111**, 756–773.

Berger, A. & Loutre, M. F. 1991 Insolation values for the climate of the last 10 million years. *Quat. Sci. Rev.* **10**, 297–317.

Berggren, W. A., Kent, D. V., Flynn, J. J. & Van Couvering, J. A. 1985 Cenozoic geochronology. *Geol. Soc. Am. Bull.* **96**, 1407–1418.

Clemens, S. C., Murray, D. W. & Prell, W. L. 1996 Nonstationary phase of the Plio-Pleistocene Asian Monsoon. *Science* **274**, 943–948.

Fairbanks, R. G. & Matthews, R. K. 1978 The marine oxygen isotope record in Pleistocene coral, Barbados, West Indies. *Quat. Res.* **10**, 181–196.

Hall, C. M. & Farrell, J. W. 1994 Laser ^{40}Ar/^{39}Ar dating of tephra in marine sediments: calibrating the geomagnetic polarity time scale. In *Proc. 8th Int. Conf. on Geochronology, Cosmochronology, and Isotope Geology*. Berkeley, CA: US Geological Survey Circular.

Hilgen, F. J. 1991*a* Astronomical calibration of Gauss to Matuyama sapropels in the Mediterranean and implication for the geomagnetic polarity time scale. *Earth Planet. Sci. Lett.* **104**, 226–244.

Hilgen, F. J. 1991*b* Extension of the astrophysically calibrated (polarity) time scale to the Miocene–Pliocene boundary. *Earth Planet. Sci. Lett.* **107**, 349–368.

Hilgen, F. J., Lourens, L. J., Berger, A. & Loutre, M. F. 1993 Evaluation of the astronomically calibrated time scale for the Late Pliocene and earliest Pleistocene. *Paleoceanography* **8**, 549–566.

Imbrie, J. & Imbrie, J. Z. 1980 Modelling the climatic response to orbital variations. *Science* **207**, 943–953.

Imbrie, J., Hays, J. D., Martinson, D. G., McIntyre, A., Mix, A. C., Morley, J. J., Pisias, N. G., Prell, W. L. & Shackleton, N. J. 1984 The orbital theory of Pleistocene climate: support from a revised chronology of the marine δ^{18}O record. In *Milankovitch and climate*, Part 1 (ed. A. L. Berger, J. Imbrie, J. Hays, G. Kukla & B. Saltzman), pp. 269–305. Hingham: D. Riedel.

Imbrie, J. (and 17 others) 1992 On the structure and origin of major glaciation cycles. 1. Linear responses to Milankovitch forcing. *Paleoceanography* **7**, 701–738.

Imbrie, J. (and 18 others) 1993 On the structure and origin of major glaciation cycles. 2. The 100,000-year cycle. *Paleoceanography* **8**, 699–735.

Laskar, J. 1990 The chaotic motion of the solar system: a numerical estimation of the size of the chaotic zones. *Icarus* **88**, 266–291.

Laskar, J., Jouzel, F. & Boudin, F. 1993 Orbital, precessional, and insolation quantities for the Earth from −20 Myr to +10 Myr. *Astron. Astrophys.* **270**, 522–533.

Lourens, L. J., Antonarakou, A., Hilgen, F. J., Van Hoof, A. A. M., Vergnaud-Grazzini, C. & Zachariasse, W. J. 1996 Evaluation of the Plio-Pleistocene astronomical time scale. *Paleoceanography* **11**, 391–414.

McDougall, I., Brown, F. H., Cerling, T. E. & Hillhouse, J. W. 1992 A reappraisal of the geomagnetic polarity time scale to 4 Ma using data from the Turkana Basin, East Africa. *Geophys. Res. Lett.* **19**, 2349–2352.

Raymo, M. E., Ruddiman, W. F., Bachman, J., Clement, B. M. & Martinson, D. G. 1989 Late Pliocene variation in Northern Hemisphere ice sheets and North Atlantic deep water circulation. *Paleoceanography* **4**, 413–446.

Ruddiman, W. F., Raymo, M. & McIntyre, A. 1986 Matuyama 41,000-year cycles: North Atlantic Ocean and Northern Hemisphere ice sheets. *Earth Planet. Sci. Lett.* **80**, 117–129.

Shackleton, N. J., Berger, A. & Peltier, W. R. 1990 An alternative astronomical calibration of the Lower Pleistocene timescale based on ODP Site 677. *Trans. R. Soc. Edinb.* **81**, 251–261.

Shackleton, N. J., Crowhurst, S., Hagleberg, T., Pisias, N. G. & Schneider, D. A. 1995*a* A new late Neogene time scale: application to Leg 138 sites. In *Proc. ODP, Sci. Results* (ed. N. G. Pisias, L. A. Mayer, T. R. Janecek, A. Palmer-Julson & T. H. van Andel), pp. 73–101.

Shackleton, N. J., Hagelberg, T. K. & Crowhurst, S. J. 1995*b* Evaluating the success of astronomical tuning: pitfalls of using coherence as a criterion for assessing pre-Pleistocene timescales. *Paleoceanography* **10**, 693–697.

Tauxe, L., Deino, A. D., Behrensmeyer, A. K. & Potts, R. 1992 Pinning down the Bruhnes/Matuyama and upper Jaramillo boundaries: a reconciliation of orbital and isotopic time scales. *Earth Planet. Sci. Lett.* **109**, 561–572.

Tiedemann, R. & Franz, S. O. 1998 Deep-water circulation, chemistry, and terrigenous sediment supply in the equatorial Atlantic during the Pliocene, 3.3–2.6 Ma and 5–4.5 Ma. *Proc. ODP, Sci. Results* **154**, 299–318.

Tiedemann, R., Sarnthein, M. & Shackleton, N. J. 1994 Astronomical timescale for the Pliocene Atlantic δ^{18}O and dust flux records of ODP Site 659. *Paleoceanography* **9**, 619–638.

Walter, R. C., Manega, P. C., Hay, R. L., Drake, R. E. & Curtis, G. H. 1991 Laser-fusion ^{40}Ar/^{39}Ar dating of Bed I, Olduvai Gorge, Tanzania. *Nature* **354**, 145–149.

Walter, R. C., Deino, A., Renne, P. & Tauxe, L. 1992 Refining the Plio-Pleistocene GPTS using laser fusion ^{40}Ar/^{39}Ar tephrochronology: case studies from the East African Rift. *Eos* (Suppl.) **73**, 629.

PHILOSOPHICAL TRANSACTIONS OF THE ROYAL SOCIETY A MATHEMATICAL, PHYSICAL & ENGINEERING SCIENCES